International Journal of Dentistry and Oral Science (IJDOS)
ISSN: 2377-8075

Optical Coherence Technology Detects Early Signs of Peri-implant Mucositis in the Minipig Model

Research Article

Bordin S[1*], Pino CM[1], Mavadia-Shukla J[2], Li X[2]

[1] Department of Periodontics, School of Dentistry, University of Washington, Seattle, Washington, USA.
[2] Departmentof Biomedical Engineering, School of Medicine, Johns Hopkins University, Baltimore, Maryland, USA.

Abstract

Background: Peri-implant mucositis defines the inflammation of gingival tissue surrounding osseous integrated implants without destruction of supporting bone. Untreated mucositis may develop into peri-implantitis with irreversible resorption of alveolar bone and implant failure. Mucositis is reversible with early intervention; however, existing clinical approaches have proved inadequate to reveal initial stages of this complication. Optical Coherence Tomography (OCT) is a non-invasive modality that provides real time, cross-sectional optical images of tissue up to 2-3mm in depth from the surface. Here, the minipig model assessed the diagnostic capability of OCT to detect early signs of mucositis by imaging microstructural changes of soft peri-implant tissue based on its correspondent histological analysis.

Methods: Implants were placed in edentulous ridges of anesthetized animals. After a 7-8 weeks healing to achieve osseous integration, peri-implant disease was induced by ligature procedures. At endpoints of 3, 7 and 12 days after ligation, implant sites were clinically examined by bleeding on probing, probing depth, clinical attachment loss, suppuration and radiographic changes in bone level. Biopsies were collected for *ex vivo* optical imaging and histological analysis.

Results: As early as 3 to 7 days after ligation, imaging documented the internal disarrangement of peri-implant gingival tissue and the images correlated well with corresponding histological specimens. Clinical signs of inflammation and loss of alveolar bone were absent.

Conclusion: Development of clinical applications of OCT imaging for early diagnosis of mucositis could lead to therapeutic interventions to reduce one of the causes of implant failure.

Keywords: Perimplant Mucositis; Optical Coherence Tomography; Soft Tissue Architecture; Swine Animal Model.

Introduction

Perimplant diseases are clinically distinct in mucositis and peri-implantitis. Mucositis identifies the soft tissue inflammation around an implant, while peri-implantitis includes the loss of the supporting alveolar bone beyond biological remodeling [1, 2]. Untreated mucositis could develop into peri-implantitis and risk of implant failure. Existing strategies are not completely effective for the cure of peri-implantitis; instead, non-surgical treatment can reverse early stages of mucositis [3]. Although early detection of mucositis is crucial to preserve the implant, accurate diagnosis of the complication is problematic since current evaluation methods differ on a wide range of clinical parameters [2, 4]. Alternative diagnostic imaging modalities, including conventional X-ray radiography, computed tomography, ultrasound, magnetic resonance imaging and spectroscopy are difficult to resolve the sub-millimeter peri-implant tissue structure and are impractical in routine clinical dentistry settings [5].

***Corresponding Author**:
Sandra Bordin PhD,
Research Professor, Department of Periodontics, University of Washington, School of Dentistry, 1959 NE Pacific Street, Box 357444, USA.
Tel: 206-543-5043
Fax: 206-616-7478
E-mail: bordin@uw.edu

Received: November 18, 2016
Accepted: December 01, 2016
Published: December 02, 2016

Citation: Bordin S, Pino CM, Mavadia-Shukla J, Li X (2016) Optical Coherence Technology Detects Early Signs of Peri-implant Mucositis in the Minipig Model. *Int J Dentistry Oral Sci.* 3(12), 375-379. **doi:** http://dx.doi.org/10.19070/2377-8075-1600076

On the other hand, the technology of Optical Coherence Tomography (OCT) has been used ex vivo and *in vivo* to image tissue disorganization at early stages of disease in various systems [6-10]. OCT is a non-invasive and non-contact optical technique that provides two-and three-dimensional high-resolution (<20-m) cross sectional images of internal tissue microstructures in situ up to 2-3-mm in depth from the surface without use of ionizing radiation, giving clinicians quantitative and qualitative information in real time (<10 seconds per image acquisition) [7, 8]. The principle is analog to pulse-echo ultrasound scanning, except light is used rather than sound to create the image. OCT imaging of the oral cavity has been proposed as a more reproducible method for determining defects of hard- and soft-tissue attachment structures in periodontitis, and as an alternative to radiographic techniques for assessing caries lesions [11-14]. OCT has never been used around dental implants as a reliable diagnostic method for preventing peri-implantitis. To date, OCT monitoring of oral mucositis has been used only to evaluate damage of the tongue of mice exposed to chemotherapy and radiation [15, 16].

This feasibility study evaluated the capability of OCT to image structural disorders of soft tissue of experimental mucositis in the minipig animal model.

Material and Methods

Animal Model

Nine skeletally mature Göttingen female minipigs (Sus Scrofa-Marshall BioResources, North Rose, NY) were treated under institutional standard operating guidelines for the care and use of laboratory animals (UW-IACUC approved protocol #2276-02).

Survival Surgery: Preoperative Protocol

Animals acclimatized in their facilities for 4-6 days. Food was withheld for 12-14 hours before anesthesia, but water was available continuously. No anti-inflammatory or antibiotic medications were administered either pre- or post- operative interventions.

Anesthesia

All procedures used aseptic techniques. After induction of general anesthesia by Telazol/xylazine (Telazol 5.5 mg/kg, xylazine 2 to 3 mg/kg) and glycopyrolate (0.005 mg/kg) injected intramuscularly (IM), the insertion of an endotracheal tube established a patent airway and animals were maintained on inhalant anesthesia (1.5% to 2.5% isofluorane and 100% oxygen). Injection in the premolar areas of 2% lidocaine with 1:100,000 epinephrine induced local anesthesia. Buprenorphine (0.01-0.02-mg/kg, IM) and a 100-mcg fentanyl patch applied for 1-week provided post-operative analgesia.

Implant Placement

Mandible edentulous ridges, adjacent canines and premolars were debrided and curetted to remove calculus, plaque, and food debris. A crestal incision was made between the canine on the mesial and the first premolar on the distal sites. Anterior and posterior vertical releasing incisions raised a full thickness muco-periosteal flap exposing the surgical area. The gingival collars around adjacent teeth were spared with parallel lines allowing for apical positioning of tissue around implants during healing. Two Straumann Standard Plus implants (3.3x10-mm RN and 4.1x8-mm TE) were placed bilaterally into the mandible ridges of each animal at a 50nCm depth. Healing abutments of 3-mm were seated on implants and 4.0 chromic gut simple interrupted sutures closed the flaps (Vicryl Rapide). Edentulous ridges on maxillas assured that implants were unopposed. Animals were monitored twice daily for 7 days following surgery for signs of gum inflammation, increase in rectal temperature (35.5 ± 0.5°C), and food abstention.

Oral Hygiene Treatment

Plaque control was provided twice a week for 7-8 weeks following implant placement by debriding the areas after sedating the animals with xylazine (2-3 mg/kg)/butorphanol (0.1-0.3 mg/kg)/telazol (2-5 mg/kg) IM.

Ligature Placement

After 7-8 weeks healing period, peri-implant disease was induced in each pig by placing 4.0 silk-ligatures around abutments of two test implants randomly chosen. Positive controls consisted of unligated implants, and negative controls of healthy adjacent canines/premolars.

Clinical Parameters

Buccal and lingual probing attachment level (PAL) and probing depth (PD) of tissues surrounding each experimental and control sites, and corresponding radiographs of supporting bone, were taken two weeks after implant placement to establish baseline at day 0, and at each endpoint to evaluate disease progression.

Sample Collection

Endpoints were set up at 3-, 7- and 12-days after ligature placement. At each endpoint, three animals were randomly euthanized with 1-ml/4.5 kg Euthasol (pentobarbital and phenytoin dose of 87-mg/kg and 11-mg/kg) respectively. Blocks of buccal gingivae (approximately 5-10 mm) were removed.

Ex vivo OCT Imaging

A prototype dental OCT imaging system (Figure 1) analyzed the biopsies according to published procedures [7-9].

Histology

Biopsies were fixed in 10% formalin for routine paraffin histology. Light microscopy analysis of sections stained with Masson's-Trichrome reagent visualized integrity of the collagen matrix and epithelium, and density of infiltrate.

Radiographic Analysis

Periapical radiographs were taken with a handheld intraoral x-ray digital system (Aribex Nomad Pro).

Descriptive Statistics

Two calibrated dentists scored the clinical data according to hu-

Figure 1. Prototype Dental OCT System.

(A) Swept-Source OCT (SS-OCT) system with a central wavelength of 1310 nm, a 150 nm bandwidth sweeping at 40 to 220kAlines/second, axial resolution ~9.7 ~m in air (i.e., ~7.0 µm in tissue), transverse resolution of ~16 µm, and detection sensitivity of 120dB. The handheld probe scans 2.0 mm transversely to acquire one cross-sectional OCT frame with imaging depth set to 2.5 mm in air. (B) Spectral Domain OCT (SD-OCT) system with a central wavelength of 820 nm, a bandwidth of 150 nm, axial resolution ~2.8 µm in air (i.e., ~2.0 µm in tissue), transverse resolution of 16 µm, and detection sensitivity is ~106dB. The laser beam scans 3.0 mm transversely with an imaging depth of 1.4 mm. Both the SS-OCT and SD-OCT systems measure the intensity profile of near-infrared light backscattered from the tissue sample. The backscattered light intensities, as a function of their axial and transverse position in the tissue, compose the final OCT images representing the optical properties of the tissue microstructures displayed in an inverted grayscale color-map. Scans of the biopsies were taken from the buccal epithelium to the implant and/or the natural roots at different depths from 0 to 1.8 mm in tissue. (C) Schematic of hand held endoscopic probe, (D) corresponding photograph for SS-OCT hand held probe for dental imaging.

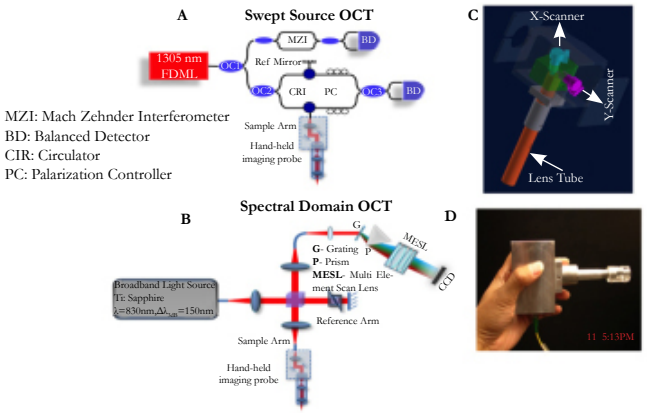

man evaluations systems [17]. Two calibrated observers examined OCT images according to quantitative imaging-scored systems. Two calibrated independent pathologists evaluated the histological features of specimens. For each category of examiners, evaluations were complete once an intra and inter-examiner concordance rate of 90% was reached. Biopsies were classified as healthy, early signs of disruption and diseased, according to clinical signs, OCT imaging and histopathology.

Results

Clinical Findings of Natural Teeth, Unligated and Ligated Implants

At 3- and 7-days endpoints, plaque formation was absent and clinically healthy mucosa surrounded each implant. Mean probing depth (PD) and attachment level (PAL) did not change compared to baseline, indicating that gingival recession was not relevant (Table 1).

No significant changes in bleeding on probing (BOP), suppuration or mobility of the fixtures were detected, and percussion testing confirmed osseo-integration. Radiographs showed implants were osseo-integrated and bone remodeling, rather than bone destruction, had occurred (Figure 2).

At the 12- days endpoint, tissues of ligated implant were inflamed and edematous with profuse BOP, increased mean PD and PAL (Table 1) and extended bone loss (data not shown) indicating that peri-implanttis had occurred.

Although clinical observations suggested absence of peri-implant complications at the 3- and 7- days endpoints,histological and OCT imaging further investigated possible internal signs of mucositis.

Histological Observations

Structural landmarks of tissues surrounding canines/premolars consisted of a thick, intact epithelial barrier (E), well defined submucosal rete ridges (RR), and organized collagen fibers (CM) in the matrix with limited infiltrates (Figure 3g). Tissues surrounding un-ligated implants, exhibited a still intact epithelial barrier, but a less-defined rete-ridges. The collagen matrix was generally organized, but more areas of infiltrates were noticeable (Figure 3h). Tissues surrounding ligated implants showed a much thinner and irregular epithelial barrier, poorly defined rete ridges, disorganization of the collagen fibers in areas contacting implant surfaces with increased density of infiltrates (I) indicating an inflammatory status (Figure 3j).

OCT Imaging

OCT images mirrored the tissue architecture of the corresponding histological sections. Premolar/canine tissues and unligated implants showed a thick, intact epithelial layer, well-defined rete-ridges and minimal infiltrates (Figure 3 a, b, d, e). However, OCT images of ligated implants revealed disruptions of the epithelial barrier, a discontinuous rete-ridges, and increased infiltrates in the matrix indicating tissue inflammation (Figrue 3).

Discussion

Peri-implant mucositis occurs in about 80% of treated patients-due to biofilm-associated infections [2]. Early diagnosis is crucial for proper treatments to maintain a patient's implant health.

Although histological examination of tissues can provide definitive and objective evaluation of implant health and disease, clinical practices do not allow the elective removal of biopsies

Figure 2. Radiographic Images of Implants at Ligature Placement (A, B); 3 Days After Ligature Placement (C,D); and 7-days after Ligature Placement (E,F).

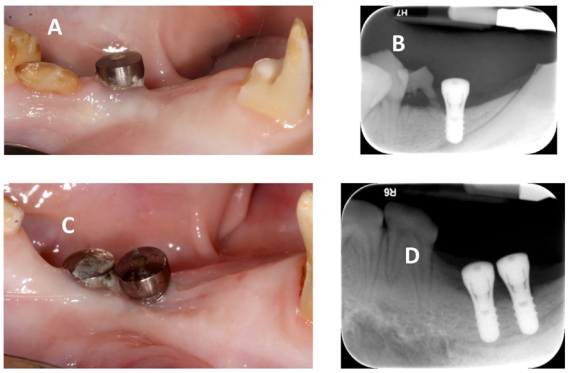

Table 1. Changes of Clinical and Radiographic Parameters Between 0-Day Baseline and 3-7-12-Days After Ligature Placement. Anova Test Analyzed Data. Bonferroni-Adjusted Student T –Test Performed Pair Wise Comparisons. NS = Not Significant Different.

Perameters	Baseline	3-Days	7-Days	12-Days
ΔPD (mm)	2.97 (± 0.2)	2.25(± 0.3)	3.08(± 0.3)	6.72(± 1.5)
ΔPAL (mm)	5.28(± 0.2)	5.67(0.5)	5.28(± 0.3)	10.88(± 2.2

Figure 3. Series of Histological Sections (g, h, j) and Corresponding *ex-vivo* High-Resolution OCT images Taken from the Same Animal for Each Condition. Representative Spectral Domain (SD-OCT) Cross-Sectional Images (a, b, c) and High-Speed Swept Source (SS-OCT) Images (d, e, f) of Gingival Tissues Surrounding Natural Teeth, Implants and Ligated Implants. (E) Epithelial Barrier, (RR) Rete-Ridges, (CM) Collagen Matrix, (I) Cellular infiltrates.

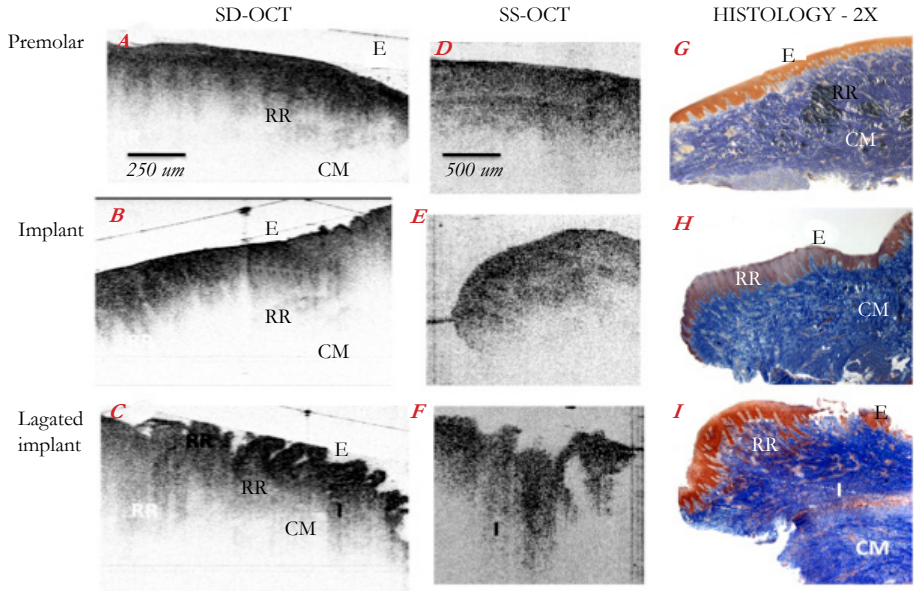

from patients. Due to inherent limitations of the human model, improvement of current guidelines for accurate diagnosis of mucositis must rely on research on animals.

Peri-implant diseases induced by ligature procedures in animals exhibit histo-pathological features in common with naturally occurring lesions in patients [18-20]. The miniature swine, which is closely species-related to man, provides a suitable dental research model for implants [19-22]. Peri-implant mucositis is of a relatively short duration window in animal models, and no reports have documented the onset of this phase in the experimental swine. This study documents that mucositis can be detected as early as 3- to 7- days after ligature induction by using OCT imaging. By day 12, mucositis had progressed to peri-implantitis with loss of the supporting alveolar bone. This time-line might facilitate designing further experiments to unravel molecular and cellular processes leading to peri-implantits.

What benefits OCT imaging and associated research add for patients and providers? The simple answer would be a decrease in health care costs since the technology will endow clinicians with a system to provide early and effective therapies and monitor treatment outcomes. However, a more comprehensive answer is that OCT affords a tool to move beyond current clinical parameters,

which may or may not be prognostic, if even diagnostic. The key benefits of OCT are: non-invasive, thus no preparation of the sample or subject is necessary: instant, direct imaging of tissue morphology at near-microscopic resolution; safe, does not involve ionizing radiations; objective and accurate diagnosis before clinical signs are noted, thus OCT could work for any operator, at any time. The technology could aid clinicians to detect and monitor structural alterations of soft periodontal tissues in a broad range of conditions. OCT is able to provide 3D volumetric imaging of tissue microarchitecture.

In summary, presented data suggest that clinical application of the non-invasive, real-time OCT imaging technology could become an objective, user-friendly tool to assess diagnosis of peri-impant complications.

Conclusion

In the minipig model, non-invasive Optical Coherence Tomography (OCTT is capable of imaging in real time early microstructural changes in soft peri-implant tissues during the development of ligature-induced mucositis. OCT data correlate well with histological features.

Acknowledgments

Research was supported by the American Association of Implant Dentistry Research Foundation and the Hack Endowment. Straumann donated the implants.

References

[1]. Lindhe J, Meyle J (2008) Peri-implant diseases: Consensus Report of the Sixth European Workshop on Periodontology. J Clin Periodontol. 35(8): 282-285.

[2]. Rosen P, Clem D, Cochran D, Froum S, McAlister B, et al., (2013) AAP Task Force on Peri-implantitis. Peri-implant Mucositis and Peri-implantitis: A Current Understanding of Their Diagnosis and Clinical Implications. J Periodontol. 84(4): 436-441.

[3]. Salvi GE, Aglietta M, Eick S, Sculean A, Lang NP, et al., (2012) Reversibility of experimental peri-implant mucositis compared with experimental gingivitis in humans. Clin Oral Implants Res. 23(2): 182-190.

[4]. Graziani F, Figuero E, Herrera D (2012) Systematic review of quality reporting, outcome measurements and methods to study efficacy of preventive and therapeutic approaches to peri-implant diseases. J Clin Periodontol. 39(12): 221-244.

[5]. Xiang X, Sowa MG, Iacopino AM, Maev RG, Hewko MD, et al., (2010) An update on novel non-invasive approaches for periodontal diagnosis. J Periodontol. 81(2): 186-198.

[6]. Regar E, Schaar JA, Mont E, Virmani R, Serruys PW (2003) Optical Coherence Tomography. Cardiovasc Radiat Med. 4(4):198-204.

[7]. Li X, Martin S, Pitris C, Ghanta R, Stamper DL, et al., (2005) High-resolution optical coherence tomographic imaging of osteoarthritic cartilage during open-knee surgery. Arthritis Res Ther. 7(2): 318-323.

[8]. Cobb MJ, Chen Y, Bailey SL, Kemp CJ, Li X (2006) Non-invasive imaging of carcinogen-induced early neoplasia using ultrahigh-resolution optical coherence tomography. Cancer Biomarkers. 2(3-4): 163-173.

[9]. Hwang JH, Cobb MJ, Kimmey MB, Li X (2005) Optical coherence tomography imaging of the pancreas: a needle-based approach. Clin Gastroenterol Hepatol. 3(7): S49-52.

[10]. Brown JS, Wang D, Li X, Baluyot F, Iliakis B, L, et al., (2008) In situ ultrahigh-resolution optical coherence tomography characterization of eye bank corneal tissue processed for lamellar keratoplasty. Cornea. 27(2): 802-10.

[11]. Colston BW Jr, Everett MJ, Da Silva LB, Otis LL, Stroeve P, et al., (1998) Imaging of hard- and soft-tissue structure in the oral cavity by optical coherence tomography. Applied Optics. 37(16): 3582-3585.

[12]. Feldchtein FI, Gelikonov GV, Gelikonov VM, Iksanov RR, Kuranov RV, Sergeev AM (1998) In vivo OCT imaging of hard and soft tissue of the oral cavity. Opt Express. 3(6): 239-250.

[13]. Otis LL, Everett MJ, Sathyam US, Colston BW Jr (2000) Optical Coherence Tomography: a new imaging technology for dentistry. Jam Dent Assoc. 131(4): 511-514.

[14]. Amaechi BT, Podoleanu AGh, Komarov GN, Rogers JA, Higham SM, et al., (2003) Application of Optical Coherence Tomography for imaging and assessment of early dental caries lesions. Laser Physics. 13(5): 703-710.

[15]. Muanza TM, Cotrim AP, McAuliffe M, Sowers AL, Baum BJ, et al., (2005) Evaluation of Radiation-induced Oral mucositis by Optical Coherence Tomography . Clin Cancer Res. 11(14): 5121-5127.

[16]. Wilder-Smith P, Hammer-Wilson MJ, Zhang J, Wang Q, Osann K, et al., (2007) In vivo Imaging of Oral Mucositis in an Animal Model using Optical Coherence Tomography and Optical Doppler Tomography. Clin Cancer Res. 13(8): 2449-2454.

[17]. Baderstein A, Nilveus R, Egelberg J (1984) Reproducibility of probing attachment level measurements. J Clin Periodontol. 11(7): 475-485.

[18]. Schwarz F, Herten M, Sager M, Bieling K, Sculean A, et al., (2007) Comparison of naturally occurring and ligature-induced peri-implantitis bone defects jn humans and dogs. Clin Oral Implants Res.18(2): 161-170.

[19]. Faggion CM Jr, Chambrone L, Gondim V Schmitter M, Tu YK (2010) Comparison of the effects of peri-implant infection in animal and human studies: Systematic review and meta-analysis. Clin Oral Implants Res. 21(2):137-147.

[20]. Kalkwarf KL, Kreici RF (1983) Effect of inflammation on periodontal attachment levels in miniature swine with mucogingival defects. J Periodontol. 54(6): 361-364.

[21]. Becker ST, Dörfer C, Graetz C, De Buhr W, Wiltfang J, et al., (2011) A pilot study: microbiological conditions of the oral cavity in minipigs for peri-implantitis models. Lab Anim. 45(3): 179-183.

[22]. Herring SW (2003) TMJ anatomy and animal models. J Muscoloskelet Neuronal Interact. 3(4): 391-394.